Piezotronic, ZnO overlaid Bragg grating organic vapors sensors

Diego Lopez-Torres, Cesar Elosua Aguado, Georgios A. Pappas, Maria Konstantaki, Argyro Klini, Alexandros Lappas, Francisco J. Arregui & Stavros Pissadakis

***Abstract*— We present a ZnO out-cladding, overlaid tilted optical fiber Bragg grating sensor, for the detection of vapors of common alcohols and acetone at concentrations lower than 25ppm, while operating at room temperature. The optical fiber sensing results indicate a chemostriction effect occurring in the ZnO layer when exposed to volatile organic compounds, which effect in turn induces shifts in the cladding, and most importantly, in the core confined, Bragg mode. The sensor exhibits maximum sensitivity of ~1pm/ppm to ethanol vapors, with exposure to other alcohol vapors (isopropanol and methanol) showing lower sensitivities; also, response to acetone vapors was traced at ~0.5pm/ppm. X-ray diffraction measurements of the ZnO nanolayer revealed that, in saturated ethanol vapors atmosphere, the poly-crystalline ZnO film undergoes a contraction by 0.6% of the interplanar distance corresponding to the (002) crystalline direction, denoting the chemostrictive effect through an underlying piezotronic mechanism. X-ray diffraction measurements and optical fiber sensing data are further correlated by numerical simulations carried out, so to study the strain interactions of the ZnO layer with the silica glass optical fiber.**

***Index Terms*— Piezotronics, Tilted optical fiber Bragg grating sensors, Volatile organic compounds, ZnO.**

I. Introduction

THE use of thin oxide films as transduction materials in the detection of gaseous substances through standard physisorption and chemisorption surface effects, is a subject attracting constant academic and industrial interest for more than 30 years [1]. The interactions facilitated at the surface of thin oxide films with oxidizing or reducing molecules, introduce electronic and structural changes, primarily confined in the close vicinity of the oxide surface [2]. The effect is manifested through a number of physical mechanisms including changes in fluorescence, resistivity, piezoelectricity and electrostriction, refractive index and optical density.

Zinc Oxide (ZnO), an n-type semiconductor, is considered to be one of the most promising materials into the detection of volatile organic compounds (VOCs) and oxidizing gasses, using a variety of physical mechanisms (including piezoelectricity) and reading out configurations [3]. The stoichiometry of oxygen into the ZnO crystalline matrix, defines in large the bandgap and defect states of the material, distinctively into its surface and volume, and the interaction of those defects with adsorbed molecules. In addition to the traditional and well-studied monitoring of the resistivity of ZnO thin films, optical detection approaches based on photoluminescence [4] and refractivity [5] processes have been correlated with interactions of the material with organic vapors of specific molecular polarity. The electronic interactions taking place onto the ZnO surface and into its depletion layer [6] with organic vapors (ketones, alcohols or halogenates), highly correlate with its photoluminescence signature by means of its spectral shape and overall intensity variations. There have been examples of photonic devices for sensing organic vapors using ZnO thin oxide films [5, 7-9] or other transductors [10], demonstrated in planar and optical fiber platforms, leading to detection figures of few ppm per volume, with some of them operating at room temperature conditions, fact that enhances their practical applicability. Nevertheless, registering, and quantifying photoluminescence is not the best route available for developing small size, portable sensing probes. Alternatively, refractive index and optical density changes of ZnO under exposure to VOCs [5] can constitute a useful approach into the development of portable and sensitive chemosensing devices [11]. In most of the above investigations of the ZnO as an optical transductor for tracing molecules of organic vapors the exact underlying sensing mechanisms are still under investigation.

We are presenting –for the first time to the best of our knowledge- chemostrictive/piezotronic organic vapor sensors based on ZnO overlayers growth onto tilted optical fiber Bragg gratings (TOFBGs). ZnO optical fiber sensing probes into the detection of alcohols or ozone have been presented before [5], however, monitoring piezotronic type of changes have been

This work was supported by the Accelerating Photonics Deployment via one Stop Shop Advanced Technology Access for Researchers (ACTPHAST 4R) project, Grant agreement ID: 825051, the Laserlab-Europe EU-H2020 871124; and in part by the Spanish Government project TEC2016-79367-C2-2-R and the Mobility program grants by Public University of Navarre.

Diego López-Torres, Cesar Elosua Aguado and Francisco J. Arregui are with the Electric, Electronic and Communication Department of the Public University of Navarre, Pamplona, 31006 Spain (email: diego.lopez@unavarra.es; cesar.elosua@unavarra.es; parregui@unavarra.es).

Georgios A. Pappas is with the Laboratory of Composite Materials and Adaptive Structures, ETH Zurich, 8092 Zurich, Switzerland (email: gpappas@ethz.ch).

Argiro Klini, Maria Konstantaki, Alexandros Lappas and Stavros Pissadakis are with the Institute of Electronic Structure and Laser (IESL), Foundation for Research and Technology Hellas (FORTH), 70013 Heraklion, Greece (email: klini@iesl.forth.gr; mkonst@iesl.forth.gr; lappas@iesl.forth.gr; pissas@iesl.forth.gr). Corresponding authors: Cesar Elosua Aguado, email: cesar.elosua@unavarra.es; Stavros Pissadakis, e-mail: pissas@iesl.forth.gr.

investigated only recently, yet not optically [12]. We apply a wet chemistry growth method of the ZnO thin film onto the FBG, while performing annealing of the ZnO overlaid gratings into oxygen rich atmosphere, improving the crystallinity of the oxide layer, and enhancing its piezotronic characteristics. The chemostrictive transduction mechanism of ZnO is monitored using a high sensitivity photonic platform that of a TOFBG [13], probing the optical and structural changes[14] introduced in the ZnO film by its interaction with the organic molecules. For further supporting, the optical fiber-based sensing results and gaining insight into the underlying transduction mechanism, we perform photoluminescence (PL), scanning electron microscope (SEM) and X-ray diffraction (XRD) measurements of the ZnO films. Furthermore, numerical simulations are carried out so to study the strain interactions occurring in the ZnO transductor.

This work aims the demonstration of a new organic vapor sensing transduction mechanism, utilizing thin oxide film technology, implemented on a powerful optical fiber platform, while exhibiting a high potential to be adopted in applications, where organic vapor detection is of utmost priority and optical fiber sensors offer unique advantage (ie vessel degassing).

II. EXPERIMENTAL

For the development of the sensor, TOFBGs were inscribed in a photosensitive single-mode low-NA fiber (GF1B–Nufern) utilizing a 193nm, 10 ns excimer laser (Braggstar, TUI laser) and a standard 1070 nm period phase mask setup [15]. For a 4º phase mask tilt angle, gratings were inscribed with enhanced cladding mode resonances observable in the 1525-1550 nm region. The gratings had a length of 5 mm, while for a repetition rate of 40 pulses/s, under the above conditions, an exposure time of approximately 6 min was required corresponding to an accumulated energy density dose of 2.6 KJ/cm^2.

Prior to any thin layer deposition, the cladding surface of the silica glass TOFBG, was functionalized to improve hydrophilicity and optimize the wet chemistry ZnO growth process. For this reason, the TOFBG was immersed into a KOH/ethanol solution for 15 minutes in an ultrasonic bath, which enhances the surface hydrophilicity and subsequently eases ZnO wet chemistry processing [16]. Zinc acetate dehydrated (obtained from Sigma Aldrich and used as it was received) was used as ZnO precursor, being dissolved in methanol, reaching a concentration of 0.152 mM [17, 18], while being stirred for 2 hours. Drop casting method was performed once to get a thin layer of the pre-cursor on the TOFBG segment and thereafter, the fiber was annealed at 300ºC for two hours (using a fixed oxygen flow rate of 0.5 l/min) to get the Zn^{2+} ions oxidized [19]. The resulting sensor was kept at room conditions for 24 hours prior to its first use. Fig.1 shows the corresponding spectral shifts Bragg, ghost [20] and cladding modes of a TOFBG as fabricated and then after the ZnO growth processing (including annealing). The growth of the ZnO film onto the cladding of the TOFBG has prominent effect in the ghost and cladding modes, leaving Bragg mode rather unaffected.

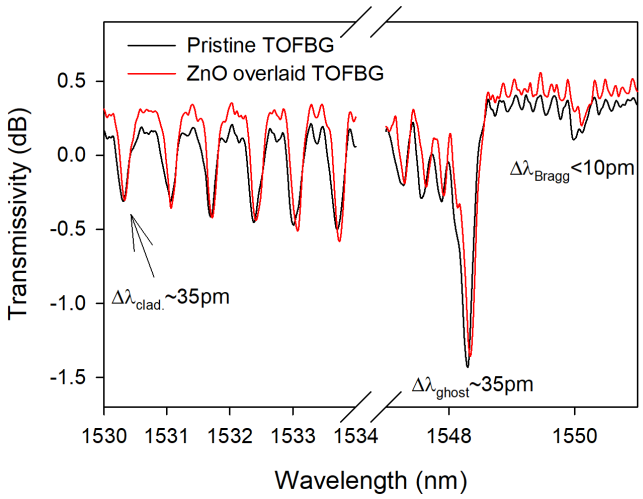

Fig. 1. Spectral shifts of core, ghost and cladding mode notches of pristine and a ¬150nm thick, ZnO overlaid TOFBG. The spectrum of the nO overlaid grating gas been obtained after the thermal annealing process at 300ºC.

SEM was used for quantifying the thickness of the ZnO deposited layer onto the optical fiber Bragg grating, revealing that under the specific casting conditions, the formation of a layer with nominal thickness of ~150nm is achieved (see Fig.2). XRD measurements performed in ZnO overlaid optical fiber samples, have shown the growth of a poly-crystalline layer on the optical fiber cladding.

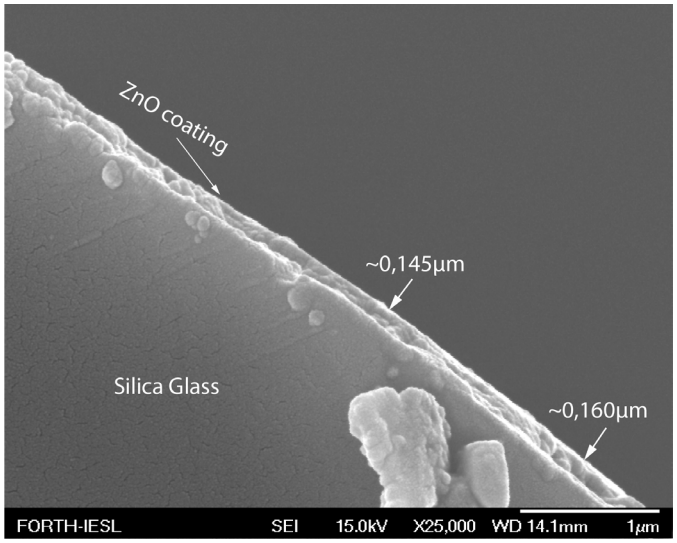

Fig. 2. SEM image from a ZnO film grown onto an optical fiber Bragg grating. The thickness of the ZnO film is estimated to be ~150nm.

In general, the use of KOH wettability functionalization improved the uniformity of the ZnO thin overlayer over the optical fiber cylindrical cladding area, while using the above liquid precursor deposition method. As it will be shown later, the improved uniformity of ZnO layer after the KOH surface functionalization, can be accounted as a positive parameter in the transduction performance of this optical sensor.

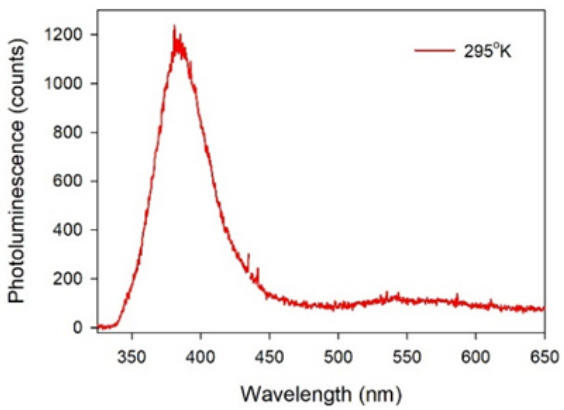

Fig. 3. Room temperature photoluminescence emission spectrum of ZnO thin film, grown onto an optical fiber Bragg grating, recorded in air upon 325 nm CW excitation.

An additional quantification of the quality of the ZnO overlaid films was obtained using photoluminescence (PL) emission measurements. The luminescence signature of ZnO films grown onto silica glass optical fibers, was recorded in ambient air at room temperature (RT), while using a system comprising of a He-Cd cw laser (325 nm, 2 mW) and a grating spectrometer (600 grooves/mm) equipped with a sensitive, liquid nitrogen-cooled CCD detector (see Fig. 3). The strong PL emission band peaking at 380 nm, is the characteristic broad near-band-edge ultraviolet emission of ZnO; also exhibiting a suppressed, long wavelength emission band centered at 550nm, being associated with reduced oxygen surface defects [2].

The ZnO based optical fiber probes were tested for their response to VOCs using a stainless steel, gas chamber with suitable gas inlets and optical fiber fit-through ports, shown in detail elsewhere [19]. The test chamber was degassed between consecutive measurements using nitrogen flow. Spectral measurements were obtained in ambient air environment after the analyte was injected in the chamber, with the devices being probed in transmission mode, using the broadband amplified spontaneous emission from an erbium doped fiber amplifier, and an optical spectrum analyser (Ando AQ6317B), at a resolution of 10pm.

III. Sensing Results

Several optical fiber sensing probes were fabricated and tested using the procedure and apparatuses mentioned above, while showing consistently similar sensing behavior. A single ZnO coated TOFBG was systematically exposed individually to methanol, ethanol, isopropanol and acetone vapors for measuring sensor sensitivity and possible hysteresis effects due to irreversible ZnO surface detachment effects. Typical concentrations of the organic vapors used, were varying between 10 and 475 ppm (v/v), covering a wide range of potential applications. Three spectral features of the ZnO overlaid OFBG were traced: the fundamental mode scattering at λ_{Bragg}=1550nm, a middle-placed cladding mode scattering at λ_{CL2}~1537.5nm, and a far scattering, cladding mode located at λ_{CL1}~1530.5nm. Typical broadband spectra of the ZnO overlaid, Bragg grating reflector before and after been exposed to acetone and ethanol vapors are presented in Fig.4.

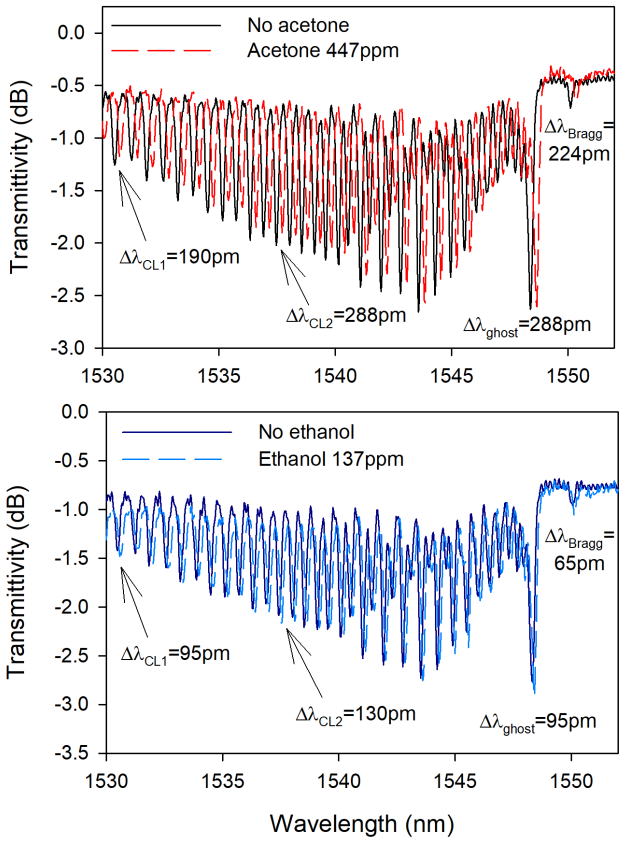

Fig. 4. Transmission spectra of a ~150nm thick ZnO film overlaid tilted optical fiber Bragg grating, before and after exposure to organic solvents. (upper) 477ppm of acetone vapors. (lower) 137ppm of ethanol vapor. All exposures have been carried out at at 22ºC. λ_{Bragg}=1550nm, λ_{CL1}=1530.52nm, λ_{CL2}=1537.47nm.

The data of Fig.4 are of particular interest: contrary to previous demonstrations (presented at [19]), the transduction of the thin ZnO during its exposures to the VOCs, results in a universal shift of all the cladding, ghost, and also surprisingly of the fundamental (Bragg) mode. Contrary to the current observations, previous studies [19] shown that the transduction between VOC and ZnO nanolayers resulted in spectral shifts solely of the cladding and ghost modes (which modally interact with the ZnO overlayer), with the fundamental mode that has no modal interaction with the sensing over-layer, remaining unchanged. Refractive index and optical loss changes occurring in the ZnO overlayer, by its exposure to organic solvent vapor, cannot justify spectral shift changes occurring in the fundamental mode of the Bragg reflector, shown here. The data of Fig.4 reveal that cladding, ghost and core modes shift differentially versus exposure to organic solvents vapors, with cladding and ghost modes exhibiting slightly greater transduction shifts than the core-confined Bragg mode.

Comparative spectral shift data of cladding and Bragg (core) mode, for exposure of the sensing probe to ethanol and acetone vapors are provided in Fig.5. The spectral shifts $\Delta\lambda_{Bragg}$ obtained for the Bragg mode of the TOFBG, after exposure to VOCs are generally smaller than those measured using cladding and ghost modes. Cladding modes undergo refractive index

changes related to the adsorption of organic vapors onto the ZnO thin film, which can be of photorefractive and/or of photoelastic nature; the core mode can only be subjected to the later one. Photorefractive changes into the ZnO films generated by ethanol adsorption have been confirmed before [5], while being related to the fundamental interaction mechanism between ZnO, oxygen molecules and the VOCs (see also discussion in section IV.C).

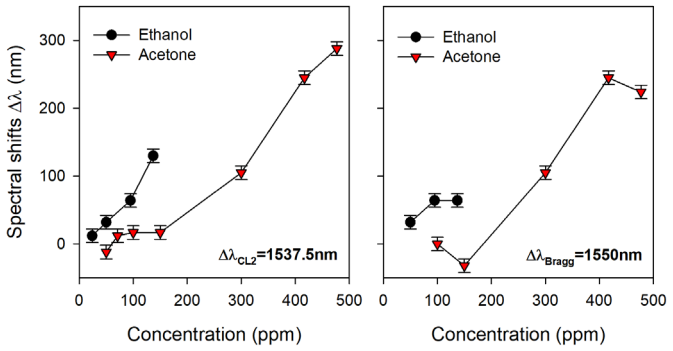

Fig. 5. Spectral shift data of cladding $\Delta\lambda_{CL2}$ and Bragg (core) $\Delta\lambda_{Bragg}$ modes of a TOFBG sensor overlaid with a 150nm thick ZnO film, after being exposed to ethanol and acetone vapors.

The sensitivity (spectral shift per VOC concentration, pm/ppm) of the sensor to different organic solvents vapors is presented in Fig.6. The ZnO based sensing probe shows distinct sensing behavior for the three different alcohols used, as well as, for acetone. Checking the data of Fig.6, one can see that the sensitivity of the probe is maximum for ethanol and isopropanol, yet negligible for methanol. This is because methanol has been used as a precursor for the wet-chemistry ZnO growth onto the optical fiber cladding, pre-passivating defect sites of the material. Accordingly, the sensitivity of the ZnO based probe to acetone rests in between the above two types of alcohols; acetone has a surface interaction mechanism with the ZnO that is underlined by its double bonded oxygen, which is structurally different than the –OH based interaction holding for alcohols. The ZnO overlaid fiber Bragg grating sensor exhibited detectivities between ~10ppm and 25ppm for the three aforementioned organic vapors (ethanol, isopropanol and acetone).

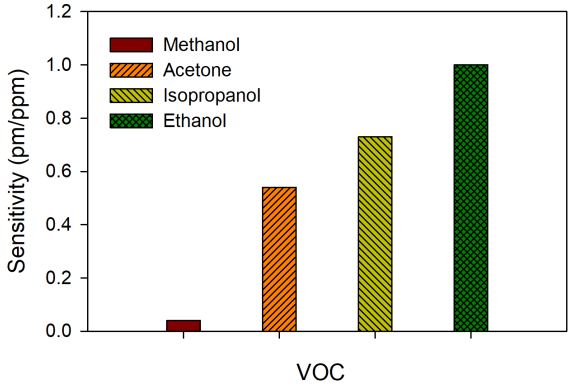

Fig. 6. Maximum sensitivity (linearized) of the ZnO overlaid TOFBG for different organic solvents vapors, estimated from the spectral shift values at the maximum vapor pressure point for each solvent.

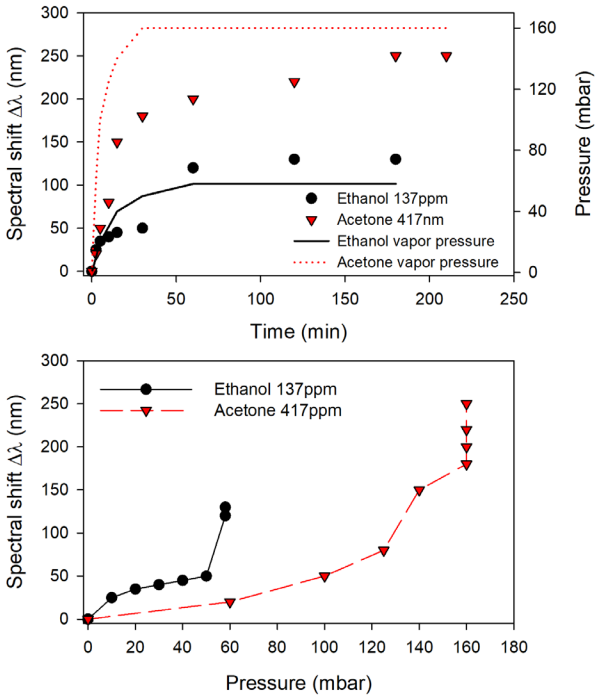

Fig. 7. Sensor response versus time (upper) and versus vapor pressure (lower) when it was exposed to different VOCs. The experimental points refer to the λ_{CL1}=1537.52nm cladding mode spectral shifts.

The temporal response of the sensing probe at saturated atmosphere for selected organic vapors investigated is presented in Fig.7: fastest temporal response factors $\Delta\lambda/\Delta t$ are 10pm/min for ethanol and 24pm/min for acetone, measured immediately after the sensor was exposed to organic vapors. An interesting feature of Fig.7 is the spectral shifts $\Delta\lambda$ for core and cladding modes commencing from gas pressure stabilization [21]. These spectral shifts evolve for prolonged durations (up to ~150 min for acetone vapors), indicating a slow stimulation process, occurring in the ZnO nanolayer. In any case, the sensing probe fully recovers its optical characteristics after being exposed to ambient air or nitrogen flow, in characteristic times similar to the rise-up times presented in Fig.7.

IV. Sensing Mechanism Elaboration

The major question rising from the optical fiber sensing, experimental results presented in this manuscript, relates to the transduction mechanism of organic vapor sensing using the ZnO overlayer. The particular sensing behavior of the ZnO overlaid fiber Bragg gratings examined here, where spectral features related to core and cladding guided modal scattering, shift simultaneously versus organic vapor stimulation, is atypical. We attribute this unique transduction performance to chemostrictive effects occurring in the ZnO nanolayer, related to its inherent piezoelectric/piezotronic properties. Interaction of the VOCs with the ZnO surface, will result in the introduction of strain effects in the thin ZnO layer, which will be then translated to the optical fiber, photo-elastically affecting core and cladding modes.

To further shed light onto the chemostriction/piezotronic

mechanism assertion, we performed two-fold investigations: initially, XRD measurements of a ZnO film while being exposed to ethanol vapors, so to identify relevant changes in its crystalline structure; and then, mechanical simulations of the ZnO overlaid optical fiber sensor to correlate the spectral shifts experimentally measured with the strain interactions occurring in the ZnO transductor. With respect to the mechanical simulations, we intentionally focused on the examination of the Bragg (core) mode, since its sensing response exclusively manifests the nature of the transduction mechanism.

A. *XRD measurements*

We carried-out XRD measurements in a ZnO film overlaid onto a silica glass sample, prepared using the same growth conditions as those used for the TOFBG reflectors. These measurements were initially carried for a ZnO film grown onto a silica substrate in ambient air, and then for the same sample, under saturated ethanol vapor pressure stimulation, while preserving the sample under a sealed PMMA dome. The results of the XRD measurements for the ZnO in pristine form and under ethanol vapor stimulation, are presented in Fig.8. The XRD data of the pristine confirm the growth of a poly-crystalline film, without a preferential plane orientation (see Fig.8a). The exposure of the ZnO nanolayer to alcohol vapors introduces a shift of ~0.2° to higher angles, to the (002) crystalline direction scattering peak, located at 34.2°, which in turn results in a contraction of the interplanar distance *d* (see Fig.8b) by ~0.6% (see Fig.8c & d).

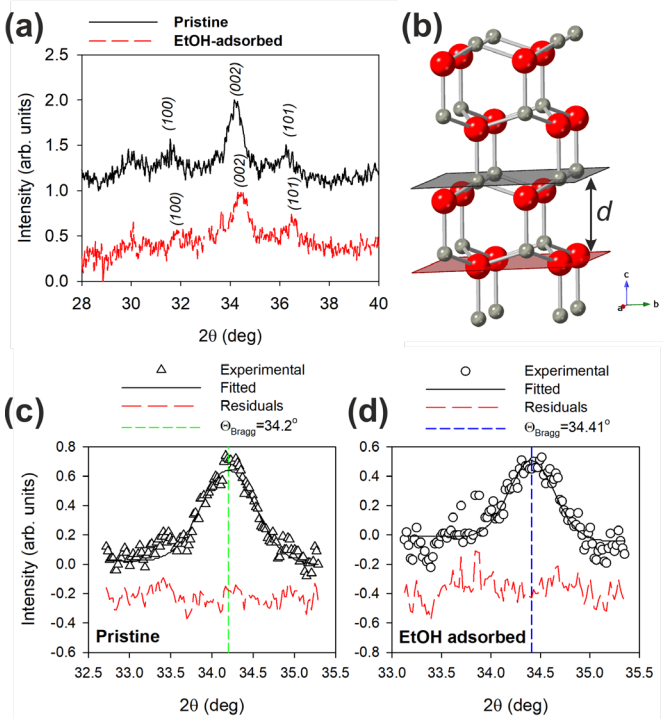

Fig. 8. (a) Background subtracted X-ray diffraction (CuKa) patterns of pristine and EtOH-activated (b) ZnO functionalised sensor; the patterns are indexed in the Wurtzite type hexagonal unit cell setting (space group P63/mc). (b) Schematic representation of the Wurtzite type crystal structure with Zn (grey) and O (red) atoms in tetrahedral coordination; a typical (002) lattice plane comprised of Zn atoms is depicted. Gaussian profile fitting of the strongest (002) reflection in the parent (c) and EtOH-activated (d) sensor.

The amount of contraction of the interplanar (002) level of ZnO thin films under the stimulation of ethanol vapors has been also observed by Kuo, et al, [22] while showing similar lattice constant changes (~0.5%). Nonetheless, from the XRD results obtained here we could not identify lattice constants shifts at other crystallographic levels. We speculate that this ethanol driven contraction predominantly along the (002) crystalline direction, is asserted as strain to the ZnO layer, which in turn is transferred to the optical fiber silica glass body.

B. *Mechanical Simulations*

Numerical simulations of the ZnO coated glass fiber system were carried out in order to study the strain interactions. All simulations were created in Abaqus 6.14 Standard environment. The coated glass fiber (GF) was modeled with the following elastic constants: E_{GF}= 70 GPa, ν_{GF}=0.16. The ZnO film was modeled with its nominal 150 nm thickness (see Fig. 2). A Poisson's ratio, ν_{ZnO}=0.358 and a Young's modulus $E_{ZnO} = 800GPa$ were implemented; the latter was measured by others using AFM indentation for high crystallinity ZnO nano-rods/layers [23], grown in thin film formats.

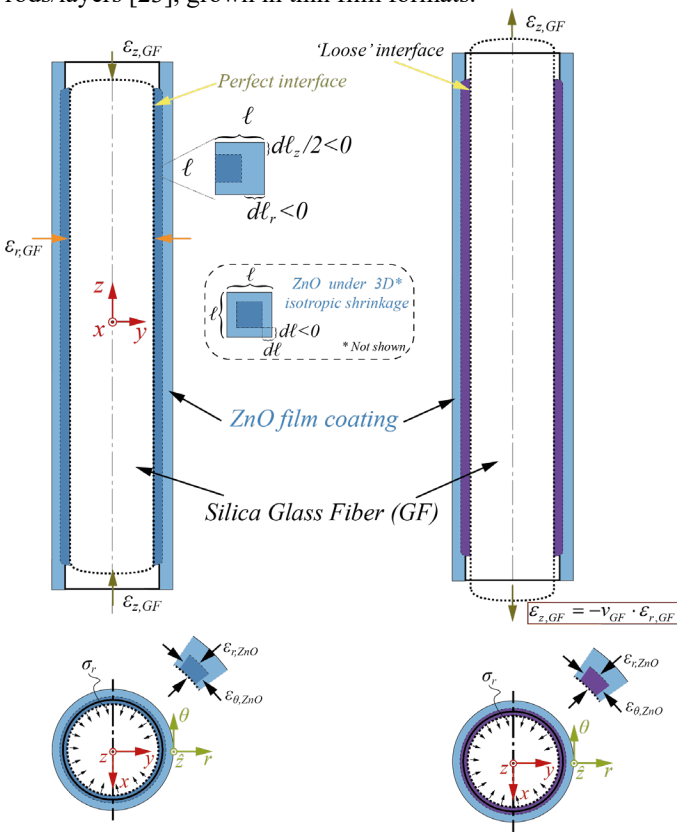

Fig. 9 Schematic (not to scale) representation of the strain interaction between the silica glass fiber and the ZnO coated film. (Left) In case of a perfect interface, the composite action prevails in all directions and for the given properties, the $\varepsilon_{z,GF}$ are resulting negative. (Right) In case of a 'loose' interface approximation, in other words when the slippage of the contributing interfaces in the axial direction (-*z*-) is not bound, then the GF is stressed in the radial direction due to the contraction of the ZnO, while on the axial direction (relating to Bragg shift) only the Poisson's effect related strains develop. Note that the two cases are the extreme bounds, but the latter is clearly closer to the actual state as corroborated by the measured Bragg shifts.

The vapor exposure effect was modelled as isotropic

shrinkage, assuming that the VOC induced electron diffusion does not exhibit specific directionality in bulk level.

Initially, an axisymmetric model with a perfect interface between glass and ZnO was built. The geometry was discretized with quadrilateral, reduced integration elements (CAX4R). A section of 1.25 mm in length was considered, being about ×10 larger than the transversal dimensions, in order to reduce any effects from the boundaries. This model showed that the shrinkage of the ZnO will take along the fiber in the axial direction (see Fig. 9) too, leading to blue shift of the Bragg mode. The last finding was in total disagreement with the experimental results.

An alternative model was attested, considering that ZnO azimuthally contracts (isotropic shrinkage) due to the interaction with organic vapors. This state was modeled using plane stress quadrilateral, reduced integration (CPS4R) elements. Under exposure to ethanol vapors, the ZnO film will cause radial stresses in the optical fiber, yet, due to the lack of composite action, the axial shrinkage of the glass fiber due to Poisson's effect can occur (see Fig. 9). The resulting stress state resembles the shrink fit equivalent problem [24]. All simulations are launched using small strain assumptions, thus, one can evaluate the equivalent Bragg peak shift $\Delta\lambda_{Bragg}$ based on the resulted axial and radial simulated strains, following Eq. 1:

$$\Delta\lambda_{Bragg} = \varepsilon_{z,GF} - \frac{n_{eff}^2}{2}\left[p_{zz}\varepsilon_{r,GF} + p_{zr}\left(\varepsilon_{r,GF} + \varepsilon_{z,GF}\right)\right] \quad (1)$$

where $\varepsilon_{z,GF}$ and $\varepsilon_{r,GF}$ axial and radial strains of the optical fiber, respectively, p_{zz} & p_{zr} the Pockel's strain–optic constants of silica glass, and n_{eff} the effective index of refraction for the guided mode [25].

The result of the last simulations relates the $\Delta\lambda_{Bragg} \approx 65pm$ recorded for ethanol vapors at saturated pressure (137ppm), to a shrinking strain on the ZnO of the order of ≈0.5%. This simulation result rests closely to the strains measured from XRD measurements for ZnO ethanol induced contraction. Differences observed may be attributed to residual strains introduced from the layer growth process, interface effects between the ZnO and the glass fiber, as well as, to no uniform strain distribution due to the depletion layer [26] of the ZnO, which is expected to be comparable to the thickness of the film.

C. *Discussion on the transduction mechanism*

In general, the interaction of organic vapors with the ZnO nanolayers, has been interpreted on the basis of redox reactions occurring between the organic analyte and oxygen molecules, absorbed onto the semiconductor's surface. Similar reasoning is behind the change of resistivity and photoluminescence emission observed in ZnO nanostructures exposed to organic vapors, while also changes in charge carrier density are important in explaining the photocatalytic activity of ZnO, as well as, the piezoelectric [27] activity of ZnO nanostructures in the presence of ethanol vapors [8]. A competing adsorption between the oxygen species and ethanol on the surface of ZnO nanostructures has also been elaborated in specific theoretical studies, as a plausable sensing mechanism [28]. This oxygen adsorption mechanism has also been proposed by other groups for describing piezotronic (but not optically traced) sensing transduction [29], for ethanol vapors tracing. In those piezotronic devices, the wurtzite-structured ZnO is under a bias compressive strain, for generating a strong piezoelectric field, along the c-axis. Electrons released during the ethanol adsorption onto the surface of ZnO, decrease its depletion zone and redistribute so to cancel out the pre-existing piezoelectric field, resulting in reversion of the bias strain [30]. A similar carrier mediated mechanism, however, employing holes holds for reduction mechanism holds for interaction with acetone vapors [31]; the last, can also explain the lower sensitivity of the ZnO to this organic solvent, attributed to the manifold lower mobility of holes compared to electrons [26].

Such a type of piezotronic transduction can also take place in the ZnO film overlaid onto the TOFBG, manifested as chemostriction that is driven by exposure of the sensor to VOCs. This chemostrictive action taking place in the ZnO film, directly affects the grating cladding modes, which overlap with the oxide film, but indirectly the Bragg mode confined in the optical fiber core, through pure photo-elastic actuation. One can question on the absence of bias strain in the ZnO overlayer [26], which is necessary for generating a strong piezopotential into the crystal [32]. Nonetheless, the growth of ZnO nanolayers onto the highly curved cladding of the silica glass optical fiber, using wet chemistry approach and subsequent high temperature crystallization annealing, can also lead to the formation of ZnO nanolayers with inherently strong piezopotential properties due to azimuthal and radial strains [33]. In our case, these curvature introduced strains are estimated to be of the order of 0.12% [33], significant enough to enhance the piezopotential properties of ZnO.

D. *Applicability note*

Beyond the elaboration of the piezotronic sensing mechanism of ZnO nanolayers as those are implemented onto optical fiber Bragg reflectors, an important point is the operation and elaboration of the specific sensing transduction into functional optical fiber sensing devices. From the data of Fig. 5, one can see that the differential spectral shift response between the core and cladding modes is limited for low organic vapor concentration. Thus, a practical sensing probe can base its operation in the monitoring of the behavior of the core mode of the ZnO overlaid Bragg grating (which purely manifests piezotronic transduction), instead of the probing of cladding modes which are affected both from photorefractive and photoelastic changes occurring in the ZnO overlayer; the last, can complicate their wavelength shift response.

An additional issue to be addressed is the cross-talk of the specific device to temperature variations. While in our case we have inscribed the Bragg grating reflectors in a standard optical fiber, one can employ typical Hi-Bi optical fibers as a grating platform [34], allowing isotropic shrinkage changes introduced by the ZnO layer, to be translated to peak splitting of the birefringent TE and TM polarization modes. In this approach, temperature variations will be de-convoluted by measuring the

total shift of the twin-Bragg peaks.

V. Summary

Our investigations on the use of ZnO nanolayers overlaid onto optical fiber Bragg gratings for the detection of vapors of organic solvents, have revealed that a chemostrictive (piezotronic) transduction mechanism takes place in the ZnO nanolayer. This mechanism affects both core and cladding modes of the optical fiber Bragg grating interrogation platform, pointing to the actuation of a strain related effect in the nanolayer, which introduces solely photo-elastic wavelength shift to the core confined Bragg mode. Additional, investigations are carried-out in order to fully correlate the optical fiber sensing data with the properties of the ZnO oxide overlayer. We anticipate that by implementing this ZnO based piezotronic transduction mechanism in smaller diameter optical fibers can lead to the development of devices with greater sensitivity; the elaboration of the same transduction mechanism in microstructured optical fibers can also be particularly interesting.

Acknowledgment

SP would like to thank Lambros Papoutsakis for performing the XRD measurements of the ZnO films, Maria Androulidaki for performing PL measurements, and Dimitrios Dolapsakis for carrying-out cladding mode simulations.

References

[1] G. Sberveglieri, "Recent developments in semiconducting thin-film gas sensors," *Sensors and Actuators B: Chemical,* vol. 23, pp. 103-109, 1995/02/01/ 1995.

[2] I. Shalish, H. Temkin, and V. Narayanamurti, "Size-dependent surface luminescence in ZnO nanowires," *Physical Review B,* vol. 69, p. 245401, 2004.

[3] Ü. Özgür, Y. I. Alivov, C. Liu, A. Teke, M. A. Reshchikov, S. Doğan, V. Avrutin, S.-J. Cho, and H. Morkoç, "A comprehensive review of ZnO materials and devices," *Journal of Applied Physics,* vol. 98, pp. -, 2005.

[4] C. Baratto, S. Todros, G. Faglia, E. Comini, G. Sberveglieri, S. Lettieri, L. Santamaria, and P. Maddalena, "Luminescence response of ZnO nanowires to gas adsorption," *Sensors and Actuators B: Chemical,* vol. 140, pp. 461-466, 2009.

[5] M. Konstantaki, A. Klini, D. Anglos, and S. Pissadakis, "An ethanol vapor detection probe based on a ZnO nanorod coated optical fiber long period grating," *Opt. Express,* vol. 20, pp. 8472-8484, 2012.

[6] M. Tonezzer, S. Iannotta, L. Dang Thi Thanh, and H. Tran Quang, "Depletion layer and dimensionality of ZnO nanostructures," in *2015 XVIII AISEM Annual Conference*, 2015, pp. 1-4.

[7] N. A. Yebo, P. Lommens, Z. Hens, and R. Baets, "An integrated optic ethanol vapor sensor based on a silicon-on-insulator microring resonator coated with a porous ZnO film," *Opt. Express,* vol. 18, pp. 11859-11866, 2010.

[8] A. Klini, S. Pissadakis, R. N. Das, E. P. Giannelis, S. H. Anastasiadis, and D. Anglos, "ZnO–PDMS Nanohybrids: A Novel Optical Sensing Platform for Ethanol Vapor Detection at Room Temperature," *The Journal of Physical Chemistry C,* vol. 119, pp. 623-631, 2015/01/08 2015.

[9] M. Śmietana, J. Grochowski, M. Myśliwiec, Ł. Wachnicki, M. Godlewski, and B. S. Witkowski, "Compact Alcohol Vapor Sensor based on Zinc Oxide Nano-coating Deposited by Atomic Layer Deposition method on Optical Fiber End-face," *Procedia Engineering,* vol. 47, pp. 1081-1084, 2012/01/01/ 2012.

[10] V. Melissinaki, O. Tsilipakos, M. Kafesaki, M. Farsari, and S. Pissadakis, "Micro-Ring Resonator Devices Prototyped on Optical Fiber Tapers by Multi-Photon Lithography," *Ieee Journal of Selected Topics in Quantum Electronics,* vol. 27, pp. 1-7, 2021.

[11] Z. Q. Zheng, J. D. Yao, B. Wang, and G. W. Yang, "Light-controlling, flexible and transparent ethanol gas sensor based on ZnO nanoparticles for wearable devices," *Scientific Reports,* vol. 5, p. 11070, 2015/06/16 2015.

[12] C. Pan, J. Zhai, and Z. L. Wang, "Piezotronics and Piezo-phototronics of Third Generation Semiconductor Nanowires," *Chemical Reviews,* vol. 119, pp. 9303-9359, 2019/08/14 2019.

[13] J. Albert, L.-Y. Shao, and C. Caucheteur, "Tilted fiber Bragg grating sensors," *Laser & Photonics Reviews,* vol. 7, pp. 83-108, 2013.

[14] T. Guo, F. Liu, B.-O. Guan, and J. Albert, "[INVITED] Tilted fiber grating mechanical and biochemical sensors," *Optics & Laser Technology,* vol. 78, pp. 19-33, 2016/04/01/ 2016.

[15] M. Konstantaki, P. Childs, M. Sozzi, and S. Pissadakis, "Relief Bragg reflectors inscribed on the capillary walls of solid-core photonic crystal fibers," *Laser & Photonics Reviews,* vol. 7, pp. 439-443, 2013.

[16] N. Chada, K. P. Sigdel, R. R. S. Gari, T. R. Matin, L. L. Randall, and G. M. King, "Glass is a Viable Substrate for Precision Force Microscopy of Membrane Proteins," *Scientific Reports,* vol. 5, p. 12550, 2015/07/31 2015.

[17] C. de Julián Fernández, M. G. Manera, G. Pellegrini, M. Bersani, G. Mattei, R. Rella, L. Vasanelli, and P. Mazzoldi, "Surface plasmon resonance optical gas sensing of nanostructured ZnO films," *Sensors and Actuators B: Chemical,* vol. 130, pp. 531-537, 2008.

[18] I. Konidakis, M. Androulidaki, G. Zito, and S. Pissadakis, "Growth of ZnO nanolayers inside the capillaries of photonic crystal fibres," *Thin Solid Films,* vol. 555, pp. 76-80, 2014/03/31/ 2014.

[19] C. Elosúa, M. Konstantaki, A. Klini, F. J. Arregui, and S. Pissadakis, *Tilted FBGs coated with ZnO nano coatings for the development of VOC sensor* vol. 11199: SPIE, 2019.

[20] L. Dong, B. Ortega, and L. Reekie, "Coupling characteristics of cladding modes in tilted optical fiber Bragg gratings," *Applied Optics,* vol. 37, pp. 5099-5105, 1998/08/01 1998.

[21] E. Navarrete, F. Güell, P. R. Martínez-Alanis, and E. Llobet, "Chemical vapour deposited ZnO nanowires for detecting ethanol and NO2," *Journal of Alloys and Compounds,* vol. 890, p. 161923, 2022/01/15/ 2022.

[22] G.-H. Kuo, H. P. Wang, H. H. Hsu, J. Wang, Y. M. Chiu, C.-J. G. Jou, T. F. Hsu, and F.-L. Chen, "Sensing of Ethanol with Nanosize Fe-ZnO Thin Films," *Journal of Nanomaterials,* vol. 2009, 2009.

[23] M. Y. Soomro, I. Hussain, N. Bano, E. Broitman, O. Nur, and M. Willander, "Nanoscale elastic modulus of single horizontal ZnO nanorod using nanoindentation experiment," *Nanoscale Research Letters,* vol. 7, p. 146, 2012/02/21 2012.

[24] R. D. Cook and W. C. Young, *Advanced mechanics of materials*, 2nd ed. ed. Upper Saddle River, N.J.: Prentice Hall ; London : Prentice Hall International, 1999.

[25] J. Botsis, "Fiber Bragg Grating Applied to In Situ Characterization of Composites," in *Wiley Encyclopedia of Composites*, ed, pp. 1-15.

[26] S. Xu, W. Guo, S. Du, M. M. T. Loy, and N. Wang, "Piezotronic Effects on the Optical Properties of ZnO Nanowires," *Nano Letters,* vol. 12, pp. 5802-5807, 2012/11/14 2012.

[27] R. K. Pandey, J. Dutta, S. Brahma, B. Rao, and C.-P. Liu, "Review on ZnO-based piezotronics and piezoelectric nanogenerators: aspects of piezopotential and screening effect," *Journal of Physics: Materials,* vol. 4, p. 044011, 2021/08/06 2021.

[28] K. K. Korir, A. Catellani, and G. Cicero, "Ethanol Gas Sensing Mechanism in ZnO Nanowires: An ab Initio Study," *The Journal of Physical Chemistry C,* vol. 118, pp. 24533-24537, 2014/10/23 2014.

[29] X. Zhang, W. Wang, D. Zhang, Q. Mi, and S. Yu, "Self-powered ethanol gas sensor based on the piezoelectric Ag/ZnO nanowire arrays at room temperature," *Journal of Materials Science: Materials in Electronics,* vol. 32, pp. 7739-7750, 2021/03/01 2021.

[30] Y. Zhao, X. Lai, P. Deng, Y. Nie, Y. Zhang, L. Xing, and X. Xue, "Pt/ZnO nanoarray nanogenerator as self-powered active gas sensor with linear ethanol sensing at room temperature," *Nanotechnology,* vol. 25, p. 115502, 2014/02/24 2014.

[31] Y. Chen, H. Zhao, B. Liu, and H. Yang, "Charge separation between wurtzite ZnO polar {001} surfaces and their enhanced photocatalytic activity," *Applied Catalysis B: Environmental,* vol. 163, pp. 189-197, 2015/02/01/ 2015.

[32] S. Niu, Y. Hu, X. Wen, Y. Zhou, F. Zhang, L. Lin, S. Wang, and Z. L. Wang, "Enhanced Performance of Flexible ZnO Nanowire Based Room-Temperature Oxygen Sensors by Piezotronic Effect," *Advanced Materials,* vol. 25, pp. 3701-3706, 2013.

[33] H. Xue, N. Pan, M. Li, Y. Wu, X. Wang, and J. G. Hou, "Probing the strain effect on near band edge emission of a curved ZnO nanowire via spatially resolved cathodoluminescence," *Nanotechnology,* vol. 21, p. 215701, 2010/04/30 2010.

[34] J. T. Kringlebotn, "Method for application of an optical fibre as a hydrostatic pressure sensor," 1999.